research articles Journal of proteome research

Analysis of Secreted Proteins as an *in vitro* Model for Discovery of Liver Toxicity Markers

John A. Lewis,* William E. Dennis, Jennifer Hadix,† and David A. Jackson

U.S. Army Center for Environmental Health Research, 568 Doughten Drive, Fort Detrick, Maryland 21702

Received June 7, 2010

Despite the wealth of sequence data and new technologies that can scan large portions of the transcriptome or proteome in a single experiment, attempts to identify human biomarkers of toxicity have been met with limited success. We have adapted an *in vitro* model system to identify proteins secreted by a human hepatoma-derived cell line (HepG2/C3A) in response to toxicant exposure. Using quantitative proteomics, we can find alterations in the abundance of proteins at the source of damage—liver cells—that are likely to be present in blood samples of exposed animals. In a proof of concept experiment, conditioned medium from cells exposed to ethanol was subjected to quantitative mass spectral analysis after abundant proteins were immunodepleted. Eighty-seven proteins were identified with almost half changing in abundance. Some of these were only identified in the highest treatment condition and presumably result from the release of intracellular proteins into the medium when the cell membrane is disrupted upon cell death. However, the majority of the identified proteins reflect known consequences of ethanol exposure or alcoholism. The analysis of proteins found in conditioned medium after exposure to toxicants appears to be a useful system for the expedited discovery of potential human biomarkers.

Keywords: ethanol exposure • HepG2/C3A • human biomarkers • liver toxicity markers • quantitative proteomics

Introduction

The genomic era has brought an unprecedented ability to analyze cellular events at a grand scale. However, the identification of markers of human disease and injury has proven difficult despite great technological advances in recent years.[1] While numerous gene expression changes have been identified using microarrays, the complexity of the data and the requirement for ribonucleic acid (RNA) from tissue samples makes these findings of limited use for clinical examination. Proteomic analysis of plasma or serum has shown more promise in identifying clinically useful markers but has been hampered because of the large number of proteins present in serum and plasma, the broad range of protein concentrations, and the dilution of tissue-specific markers.[1] Methods for identifying proteins released directly from injured tissue should yield markers specific for the injury that permit quantitative assessment of the extent and progression of the insult. Since the liver is the principal organ of detoxification and is at risk of injury from both new drug candidates and environmental chemicals,[2] an *in vitro* model that could be used for rapid identification of hepatoxicity and toxicant- or mechanism-specific biomarkers would be useful.

The set of proteins secreted from hepatocyte-derived cultured cells after exposure to toxic chemicals is likely to approximate that secreted by human liver cells into the blood. The potential protein biomarkers released by the cells into the medium in which they are grown should be at higher concentrations than in serum or plasma, and the complexity of the total protein matrix will be much lower, facilitating biomarker identification. Since primary hepatocytes are currently considered to be the standard for liver toxicology and pharmacology studies,[3] we considered using them for a secretome model system. However, because of interindividual variability and complications in culture conditions in the primary cell model, including failure to attach and limited survival time, we selected an immortalized cell line that displays a hepatocyte-like phenotype.[4]

The HepG2 cell line is a common *in vitro* model for human hepatoxicity, even though it exhibits limited ability to bioactivate toxicants[5,6] and expresses a high level of alpha-fetoprotein, which is not normally expressed by adult hepatocytes and characterizes transformed and carcinogenic hepatocyte-derived cells. A clonal isolate (HepG2/C3A) has been selected that displays a phenotype more closely resembling that of normal adult hepatocytes than the parent cell line.[7,8] In particular, HepG2/C3A bioactivates a number of chemicals, showing contact inhibition of cell proliferation and a reduction in the ratio of secreted alpha-fetoprotein to albumin when contact-inhibited.[7−9] This cell line performs liver-specific metabolic functions so well that it has been tested in a liver assist device for temporary support of patients with failing livers.[10] We expected that these characteristics would make the secretome

* To whom correspondence should be addressed. Phone: 301-619-7209. Fax: 301-619-7606. E-mail: john.a.lewis1@us.army.mil.

† SAIC, Inc., 568 Doughten Dr., Fort Detrick, MD 21702.

10.1021/pr1005668

Published on Web 09/07/2010

Report Documentation Page

Form Approved
OMB No. 0704-0188

1. REPORT DATE	2. REPORT TYPE	3. DATES COVERED
07 SEP 2010	**Research**	**01-03-2008 to 31-05-2009**

4. TITLE AND SUBTITLE
Analysis of Secreted Proteins as an in vitro Model for Discovery of Liver Toxicity Markers

5a. CONTRACT NUMBER

5b. GRANT NUMBER

5c. PROGRAM ELEMENT NUMBER
622787

6. AUTHOR(S)
John Lewis; William Dennis; Jennifer Hadix; David Jackson

5d. PROJECT NUMBER
7190

5e. TASK NUMBER
3.N

5f. WORK UNIT NUMBER

7. PERFORMING ORGANIZATION NAME(S) AND ADDRESS(ES)
U.S. Army Center for Environmental Health Research,568 Doughten Drive,Fort Detrick,MD,21702-5010

8. PERFORMING ORGANIZATION REPORT NUMBER

9. SPONSORING/MONITORING AGENCY NAME(S) AND ADDRESS(ES)
U.S. Army Medical Research and Materiel Command, 504 Scott Street, Fort Detrick, MD, 21702-5012

10. SPONSOR/MONITOR'S ACRONYM(S)
USAMRMC

11. SPONSOR/MONITOR'S REPORT NUMBER(S)

12. DISTRIBUTION/AVAILABILITY STATEMENT
Approved for public release; distribution unlimited

13. SUPPLEMENTARY NOTES

14. ABSTRACT
Despite the wealth of sequence data and new technologies that can scan large portions of the transcriptome of proteome in a single experiment, attempts to identify human biomarkers of toxicity have met with limited success. We have adapted an in vitro model system to identify proteins secreted by a human hepatoma-derived cell line (HepG2/C3A) in response to toxicant exposure. Using quantitative proteomics, we can find alterations in the abundance of proteins at the source of damage--liver cells--that are likely to be present in blood samples of exposed animals. In a proof of concept experiment, conditioned medium from cells exposed to ethanol was subjected to quantitative mass spectral analysis after abundant proteins were immunodepleted. Eighty seven proteins were identified with almost half changing in abundance. Some of these were only identified in the highest treatment condition and presumably result from the release of intracellular proteins into the medium when the cell membrane is disrupted upon cell death. However, the majority of the identified proteins reflect known consequences of ehanol exposure or alcoholism.

15. SUBJECT TERMS
ethanol exposure, HepG2/C3A, human biomarkers, liver toxicity markers, quantitative proteomics

16. SECURITY CLASSIFICATION OF:			17. LIMITATION OF ABSTRACT	18. NUMBER OF PAGES	19a. NAME OF RESPONSIBLE PERSON
a. REPORT	b. ABSTRACT	c. THIS PAGE			
unclassified	**unclassified**	**unclassified**	**1**	**9**	

of HepG2/C3A cells a valuable model for discovery of protein biomarkers of toxic exposure.

To explore the usefulness of the analysis of the HepG2/C3A secretome for the discovery of secreted protein biomarkers, we tested the well-studied hepatotoxicant, ethanol. The liver is the primary site of ethanol detoxification and is the organ most susceptible to damage. The injury appears to result from reactive oxygen species (ROS) formed during detoxification reactions.[11] An increase in lipopolysaccharides (LPS) originating from the gut in response to ethanol consumption can act synergistically to worsen the damage.[12] The effect of ethanol on the liver has been termed alcoholic liver disease (ALD), which includes a continuum of effects from inflammation and fatty liver through fibrosis and cirrhosis.[13] Hepatic inflammation is triggered by inflammatory cytokines in response to ROS and LPS. Continuous insult can lead to apoptotic or necrotic cell death and eventually to fibrosis, which appears to be part of the normal healing process and is reversible.[14] Cirrhosis is permanent damage in which healthy hepatic tissue is replaced by scar tissue and reduction in liver function is observed. Currently, liver biopsies are the standard method for measuring progression of liver fibrosis and cirrhosis. Though extensively studied, no noninvasive markers have been identified that sufficiently characterize disease progression.[15]

In this study, an in-depth analysis of the secretome of HepG2/C3A cells exposed to a model liver toxicant, ethanol was performed. An immunodepletion technique designed for serum samples was used to reduce the abundance of high-concentration secreted proteins (albumin for example) and to increase the dynamic range of the analysis. A total of 87 proteins were identified, and 27 of those changed in abundance in response to ethanol treatment. While a portion of the proteins represented cell leakage, the rest were consistent with the known effects of ethanol exposure or alcoholism, including an acute-phase response, inflammation, and changes in the extracellular matrix. This work shows that the secretome of HepG2/C3A cells provides a rich resource for identification of markers of toxic exposure.

Experimental Procedures

Maintenance Cell Culture Conditions. HepG2/C3A (ACTIV-Tox) cells were obtained from Stem Cell Innovations (SCI; Houston, TX). Cells were plated at 115 000 cells/cm^2 in Nunclon T-75 flasks (Nalgene) and grown in MED6 medium (SCI) supplemented with 5% calf serum (Hyclone) at 37 °C in 5% CO_2. Cells became confluent at about one week and were passed after two weeks per SCI's recommendations.

Exposures. For secretome analysis, HepG2/C3A cells were plated in 4 mL MED6 supplemented with 5% calf serum in 6-well plates. They were allowed to mature after reaching confluence and were only used between one and three weeks after plating. Immediately prior to exposure, cells were washed twice with serum free medium. Then MED6 (without serum) containing 200 mM, 500 mM, or no ethanol was placed on the cells. Four biological replicates were performed for each condition. Exposures were continued for 24 h. Conditioned medium containing secreted proteins was collected from each condition, centrifuged, flash frozen, and stored at −80 °C.

Protein Identification from Gel Slices. Proteins were separated using a NuPAGE Novex 4−12% Bis-Tris gel under reducing conditions and stained with the Colloidal Blue Staining Kit (Invitrogen Corp.; Carlsbad, CA) according to manufacturer's instructions. Proteins were concentrated (see "Mass spectrometry") prior to analysis. The amount of secretome loaded per lane was equivalent to 100 μL of collected media for total proteins and 130 μL for immunodepleted and column bound proteins (see "Immunodepletion").

Gel slices were manually excised, rinsed in water, and dehydrated with acetonitrile (ACN). The samples were reduced and alkylated prior to addition of 0.1% RapiGest (Waters; Milford, MA) and trypsin. After an overnight digestion at 37 °C, peptides were extracted in multiple steps using ACN solutions and 1% formic acid. The pooled extracts were dried under vacuum in an Eppendorf Concentrator 5301 (Eppendorf, Westbury, NY), reconstituted in 1% formic acid, and clarified using a 0.22 μm spin filter.

Immunodepletion. Samples were immunodepleted using the Agilent Multiple Affinity Removal System (MARS) LC Column - Human 7 system (Agilent; Palo Alto, CA), which removes albumin, IgG, IgA, transferrin, haptoglobin, antitrypsin, and fibrinogen. Secretome samples were first concentrated to less than 300 μL using a 5K Molecular Weight Cut-Off (MWCO) spin filter (Agilent, Santa Clara, CA) and brought up to 2 mL with MARS Buffer A. Samples were separated using an Agilent 1100 series High Performance Liquid Chromatography (HPLC) equipped with the MARS column maintained at 22 °C. The injection volume was 1.6 mL. Sample was loaded in 100% Buffer A at 250 μL/min. After 29 min, the eluent was switched to 100% MARS Buffer B for 7.5 min. Time-based fractions were collected, and those corresponding to peaks for unbound proteins (Buffer A) or eluted proteins (Buffer B) were pooled, creating two fractions for each sample. MARS Fraction 1 is the immunodepleted sample and MARS Fraction 2 contains the bound high-abundance proteins. Approximately half of each MARS fraction was concentrated using a 5K MWCO spin filter with a buffer exchange to 50 mM ammonium bicarbonate.

Reverse-Phase Fractionation. The remaining half of MARS Fraction 1 was further fractionated as intact proteins by direct injection onto an Agilent 1100 series HPLC equipped with an mRP-C18 High-Recovery Protein Column (4.6 × 50 mm), with the column maintained at 40 °C. A separation gradient was performed with increasing ACN concentrations and constant formic acid (0.1%) as follows: start 1% ACN to 6 min, 95% ACN at 15−25 min, 3% ACN at 25.1−30.0 min, and a 10 min post-time with 1% ACN. Eight time-based fractions (1 min each) were collected starting at 12 min and dried under vacuum in an Eppendorf Concentrator 5301. The dried fractions were reconstituted and denatured in 50 mM ammonium bicarbonate, 5 mM dithiothreitol, and 0.1% RapiGest prior to alkylation with iodacetamide (30 mM final). The sample was digested with trypsin overnight at 37 °C. Formic acid (1.5% final) was added to degrade the RapiGest, and the resultant precipitate was removed using a 0.22 μm spin filter.

Mass Spectrometry. The peptides from gel slices, MARS Fraction 2, and reverse-phase fractionated MARS Fraction 1 were separated using a Waters nanoACQUITY UltraPerformance Liquid Chromatography (UPLC) System fitted with a Symmetry C_{18} 180 μm × 20 mm, 5 μm particle size trapping column and a Bridged Ethyl Hybrid (BEH) C_{18} 100 μm × 100 mm, 1.7 μm particle size analytical column (Waters). The analytical column was maintained at 35 °C. An ACN gradient with 0.1% formic acid was used as follows: initially 1% ACN, 5% ACN at 4 min, 40% ACN at 125 min, 85% ACN at 126−131 min, 1% ACN at 132 min, and the analysis stopped at 139 min. The flow rate was 0.4 μL/min. Column elution was coupled to a Waters Q-Tof Premier quadrupole, orthogonal acceleration

time-of-flight tandem mass spectrometer. The peptides were ionized using electrospray ionization in positive ion mode. Data was collected using Waters LC-MS^E method[16] over the 50−1900 m/z range in V-mode with 0.8 s scans. Scans were performed with the collision cell voltage set at 4 V for low energy and ramped from 20 to 40 V for high energy. [Glu1]-fibrinopeptide B was used as an external lock mass for accurate mass calculations (m/z = 785.8426); a 1 s lock mass scan was collected every 30 s.

Mass spectrometry data was processed using ProteinLynx Global SERVER (PLGS) version 2.3 (build 23) with Expression version 2 (Waters).[16,17] Data preparation parameters were set to the manufacturer's default with the exception of a 785.8426 lock mass for charge 2 and 813.3895 for charge 1. Workflow parameters for database searches were set to the manufacturer's default (including automatic for precursor and fragment mass tolerance, a minimum of 3 ions per peptide, a minimum of 7 ions per protein, a minimum of 1 peptide per protein, and allowing 1 missed cleavage) with the exceptions of setting the false positive rate parameter being to 10%, allowing deamidated asparagine and glutamine and oxidated methionine as variable modifications, and enabling PPM calc (which performs a second search using a readjusted mass calibration based on the calculated masses of multiple high-scoring identified peptides). The calculated precursor mass tolerances were 10.7 ± 0.15 ppm and fragment mass tolerances were 26.7 ± 0.39 ppm. An in-house protein identification database was created from all 43 870 human RefSeq sequences (downloaded from the National Center for Biotechnology Information [NCBI] March 24, 2008) combined with likely contaminant proteins including porcine trypsin and 26 high-abundance bovine serum proteins. From gel slices, only the top-scoring protein was reported, except in the case of the albumin (ALB) and alpha-fetoprotein (AFP) gel bands (see Supporting Information for the list of identified peptides). For the bound fraction and the immunodepleted protein fractions, we reduced the overall false discovery rate for identification to less than 1% (unpublished observation based on previous searches of a database containing an equal number of randomized peptide sequences) by accepting only proteins identified in at least two replicates of any fraction of any condition (see Supporting Information for protein identification data for the bound fraction and immunodepleted protein fractions). Since it can be difficult to unambiguously identify closely related proteins such as splicing isoforms or very similar paralogs which share identical peptides, proteins were placed into a "homology group" containing a set of related proteins based on homologues identified in the ion accounting output from PLGS. Eighty-seven homology groups were identified in the reverse-phase fractionated samples.

To quantify these proteins (87 homology groups), a second database search was performed with the false positive rate parameter in PLGS set to 100%. In essence, this procedure relies solely on numeric parameters such as mass tolerance and number of ions for determining protein identifications thereby increasing the density of coverage of quantitative values for these polypeptides. The sum of the ion intensities for the three most intense peptides for each protein in the 87 homology groups was then used for quantification[18] (see Supporting Information for a complete listing of protein intensities). The coefficient of variation (CV) was calculated for each protein per each condition in which it was identified in at least three replicates, and the geometric mean CV was 27.2% for all the identified proteins. On the basis of this level of variance, an initial cut of proteins changing by 1.5 fold in any fraction were kept. For final quantification, the average ion intensity for all the fractions was summed, and the proteins whose abundance changed by 1.5 fold were reported. Because we calculated and filtered the protein changes in two ways (within fraction and total intensity) and knowing the mean CV (27.2%) for repeated measurements, we feel that the 1.5 fold cutoff is a reasonable compromise between measurement reliability and accumulating an inclusive list of proteins that are changing in abundance. Proteins identified in all four replicates of one condition but absent in others were considered to differ qualitatively between conditions. When one member of a homology group was identified in more fractions than the other possible proteins, only the most frequently identified protein is reported.

Protein Quantification. Quantibody Custom Arrays (RayBiotech; Inc., Norcross, GA) were used for multiplexed quantification of a select set of proteins. The proteins and concentration of standards are indicated: IFN-γ (25−2000 pg/mL), IGFBP-1 (247−20,000 pg/mL), IL-10 (12−100 pg/mL), IL-12 p70 (6−500 pg/mL), IL-1α (25−2,000 pg/mL), IL-1β (12−1000 pg/mL), IL-4 (25−2000 pg/mL), IL-6 (25−2000 pg/mL), MIF (2.5−200 ng/mL), and TNF α (25−2000 pg/mL). All procedures were carried out according to manufacturer's recommendations. All samples were analyzed neat and with 1/5 and 1/100 dilutions. Slides were scanned using a GenePix 4200AL Scanner (Molecular Devices; Sunnyvale, CA). Quantibody Custom Arrays contain four technical replicates for each protein measurement. To remove outliers of these replicate spots, an average CV (11.82%) was calculated by determining within technical replicate CVs for all the data and averaging it across all the samples and proteins. A 95% confidence limit was determined based on the average CV and the mean of the four technical replicates for each protein of each sample. Spots outside this limit were excluded from the analysis. Standard curves were fit to a second order polynomial using OriginPro 7 (OriginLab; Northampton, MA). No data is reported for IFN-γ because its standard curve failed or for IL-12 which was below the limit of detection. Samples were grouped by biological replicate to perform paired t tests and determine significance.

Bioinformatic Analysis. Protein annotations were obtained using Ingenuity Pathway Analysis 7.1 using content version 2002, dated 2009−02−04 01:27:32 (Ingenuity Systems, Inc.) and Entrez Gene at the National Center for Biotechnology Information (http://www.ncbi.nlm.nih.gov). An unsupervised gene ontology analysis was performed using the Database for Annotation, Visualization and Integrated Discovery (DAVID) 2008 functional annotation tool (http://david.abcc.ncifcrf.gov[19,20]). A list of 39 accession numbers, including one isoform for each gene, was submitted to DAVID. Two accession numbers were included for two of the proteins, C4 and MT, corresponding to C4A, C4B, MT1E, and MT2A. For PGAM, only the PGAM4 accession number was included. An annotation chart was generated using Gene Ontology terms levels 4 and 5 for Biological Process, Molecular Function, and Cellular Component. The Benjamini-Hochberg false discovery rate (FDR) calculated by DAVID is reported.

Results

A series of proteomic experiments was undertaken to determine the usefulness of proteins secreted from the human hepatocyte-derived HepG2/C3A cell line as a model system for identifying markers of liver toxicity. In this proof of concept work, we attempted to identify potential biomarkers of ethanol

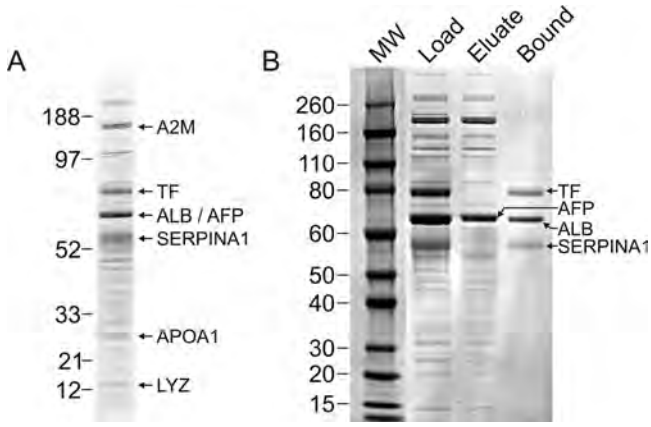

Figure 1. SDS-PAGE of HepG2/C3A secreted proteins. (A) Proteins secreted by HepG2/C3A were separated by SDS-PAGE, and several of the more intensely stained protein bands were excised and identified by mass spectrometry. Identified proteins include alpha-2-macroglobulin (A2M), transferrin (TF), albumin (ALB), alpha-fetoprotein (AFP), alpha-1-antitrypsin (SERPINA1), apolipoprotein A-1 (APOA1), and lysozyme. (B) Secreted proteins were subject to immunodepletion by column chromatography. Column load, eluate, and bound proteins are indicated. Molecular weight (MW) standards are given in kDa.

exposure or effect. Secreted proteins present in conditioned medium from ethanol-exposed and control cells were analyzed by mass spectrometry. To improve detection limits and protein identification, high-abundance secreted proteins were immunodepleted from the medium prior to trypsinization and quantitative mass spectral analysis.

Depletion of High-Abundance Proteins. A number of high-abundance proteins dominate the secretome of HepG2/C3A cells. Samples were visualized by SDS-PAGE (Figure 1A) and the most intensely staining bands were excised and subjected to mass spectral analysis. The most intense band contains albumin and alpha-fetoprotein; transferrin, antitrypsin, lysozyme, alpha-2-macroglobulin, and apolipoprotein A were also found to produce strongly staining bands (Figure 1A and Table 1). Since many of the highly abundant proteins identified in the secretome also complicate serum proteome analysis, we considered that immunodepletion methods designed for use in human serum might be well-suited for use with conditioned medium. It is clear from SDS-PAGE analysis (Figure 1B), that immunodepletion is effective in reducing the concentrations of albumin, transferrin, and antitrypsin. However, transferrin is identified in the high-ethanol concentration of the immunodepleted and fractionated analysis (see "Secretome of ethanol-treated cells"), which is likely a result of exceeding the binding capacity of the MARS column for transferrin. Alpha-fetoprotein is not removed by the column.

Mass spectral analysis of the proteins retained by the immunodepletion column revealed six proteins: transferrin, albumin, antitrypsin, antichymotrypsin, galectin 3 binding protein, and alpha-2-glycoprotein (Table 2). The presence of antichymotrypsin, galectin 3 binding protein, and alpha-2-glycoprotein was unexpected and is likely the result of nonspecific binding or cross-reactivity with the column matrix. The low signal intensities of these proteins in the mass spectra and their apparent absence by SDS-PAGE suggest that they are present only at a low concentration. Alternatively, they may

Table 1. Proteins Identified in Gel Bands[a]

symbol	name	accession number	MW (Da)	PLGS score	matched peptides	sequence cover (%)
A2M	Alpha-2-macroglobulin	NP_000005.2	163188	7978	71	63
TF	Transferrin	NP_001054.1	76999	5693	47	76
ALB	Albumin	NP_000468.1	69321	5515	38	73
AFP	Alpha-fetoprotein	NP_001125.1	68633	3034	21	58
SERPINA1	Serine proteinase inhibitor, clade A, member 1 (antitrypsin)	NP_000286.3 NP_001002235.1 NP_001002236.1	46707	7012	26	67
APOA1	Apolipoprotein A-I	NP_000030.1	30758	7363	23	73
LYZ	Lysozyme	NP_000230.1	16526	5164	6	51

[a] Bands from an SDS-PAGE analysis of proteins secreted from HepG2/C3A cells (see Figure 1) were excised and analyzed by LC−MS^E. Human Gene Nomenclature Committee (HGNC) gene symbols, National Center for Biotechnology Information (NCBI) accession numbers, and ProteinLynx Global SERVER (PLGS) scores for protein identifications have been provided.

Table 2. Proteins Bound to Immunodepletion Column

symbol	name	accession number	PLGS score	matched peptides	sequence cover (%)
TF	Transferrin	NP_001054.1	3030	46	53
ALB	Albumin	NP_000468.1	2195	37	49
SERPINA1	Serine proteinase inhibitor, clade A, member 1 (antitrypsin)	NP_000286.3 NP_001002236.1 NP_001002235.1	645	10	23
LGALS3BP	Lectin, galactoside-binding, soluble, 3 binding protein	NP_005558.1	613	10	15
SERPINA3	Serpin peptidase inhibitor, clade A, member 3 (antichymotrypsin)	NP_001076.2	423	16	37
AZGP1	Alpha-2-glycoprotein 1, zinc-binding	NP_001176.1	187	6	23

Proteins secreted by HepG2/C3A cells were collected from conditioned medium and highly abundant proteins were immunodepleted using column chromatography. The fraction that bound to the immunodepletion column was analyzed by LC−MS^E. HGNC gene symbols, NCBI accession numbers, average PLGS scores for protein identifications, average number of peptides matched per identification, and average percentage of sequence coverage per identification are provided for the identified proteins.

Table 3. Intracellular Proteins Changing in Abundance

symbol	name	biological role	200 mM	500 mM
ALDOA	Aldolase A, fructose-bisphosphate	Glycolysis/gluconeogenesis	1.91	11.92
ALDOC	Aldolase C, fructose-bisphosphate	Glycolysis/gluconeogenesis		EtOH Only
ENO1	Enolase 1	Glycolysis/gluconeogenesis	1.79	10.48
LDHA	Lactate dehydrogenase A	Glycolysis/gluconeogenesis	1.11	3.90
MDH1	Malate dehydrogenase 1	Glycolysis/gluconeogenesis		EtOH Only
PGAM	Phosphoglycerate mutase	Glycolysis/gluconeogenesis		EtOH Only
PGK1	Phosphoglycerate kinase 1	Glycolysis/gluconeogenesis	3 reps	EtOH Only
TPI1	Triosephosphate isomerase 1	Glycolysis/gluconeogenesis	0.96	4.56
GOT1	Glutamic-oxaloacetic transaminase 1 (AST)	Metabolic enzyme	1.03	4.32
FKBP1A	FK506 binding protein 1A	Apoptosis	1 rep	EtOH Only
PEBP1	Phosphatidylethanolamine binding protein 1	Apoptosis		EtOH Only
PPIA	Peptidylprolyl isomerase A	Apoptosis		EtOH Only
CFL1	Cofilin 1	Regulation of apoptosis		11.49
HSPD1	Heat shock 60 kDa protein 1	Regulation of apoptosis	2.09	9.63
HSPE1	Heat shock 10 kDa protein 1	Regulation of apoptosis	1.50	11.89
NME1	Nonmetastatic cells 1, protein	Regulation of apoptosis		EtOH Only
NME2	Nonmetastatic cells 2, protein	Regulation of apoptosis		EtOH Only
MT	Metallothionein	Oxidative stress response		EtOH Only
PARK7	Parkinson disease (autosomal recessive, early onset) 7	Oxidative stress response	1 rep	EtOH Only
PFN1	Profilin 1	Regulation of actin polymerization		EtOH Only

Proteins collected from the conditioned medium of HepG2/C3A cells treated with 200 mM ethanol, 500 mM ethanol or as control were analyzed by LC−MS^E. Proteins changing in abundance by 1.5-fold from control or identified in all four replicates of one condition but no replicates of another and annotated as being intracellular were selected. HGNC gene symbols and ratios of fold change versus control for 200 or 500 mM ethanol exposure are indicated. Proteins indentified only in exposed samples are indicated as "EtOH Only" when present in all four replicates or as the number of replicates (rep) that the protein was identified in.

be false identifications since their PLGS scores are lower than the three expected proteins, though we do not favor this idea.

Secretome of Ethanol-Treated Cells. HepG2/C3A cells were treated with 200 mM or 500 mM ethanol or left untreated; concentrations were chosen to elicit a mild to moderate cytotoxic response based on an LDH assay (approximately 10 and 35% effect, respectively; unpublished data). The medium containing secreted proteins was harvested at the end of 24 h, and highly abundant proteins were removed by immunodepletion. The depleted fraction from these samples was further fractionated using reverse-phase chromatography prior to mass spectral analysis. When we compared these fractions of the conditioned medium, we found that the abundance of 37 proteins differed between control cells and cells exposed to ethanol. While approximately two-thirds of these proteins were present in multiple conditions allowing quantitative comparison, we also found some proteins that appeared to be present only in the medium from either exposed or control cells (see "Proteomic methods"). The proteins were categorized as either intracellular (Table 3) or extracellular (Table 4). Intracellular proteins are likely to reflect "leakage" of proteins from damaged or dying cells while extracellular proteins are presumed to be secreted and to represent a physiological response to ethanol exposure.

The 20 intracellular proteins (Table 3) include a large number of glycolytic enzymes, which are some of the most abundant soluble proteins in the cytosol.[21] However, it is worth noting that the expression of some of these proteins might actually be increased as a response to the ethanol exposure since eight of them play roles in apoptosis and two (PARK7 and metallothionein) increase in response to oxidative stress[22,23]

All of the extracellular proteins in Table 4 are involved in biological processes that are known to be affected by ethanol exposure.[24,25] The majority (11 of 17) of these proteins is involved in the overlapping biological processes of the acute-phase response, inflammatory response, and apoptosis. Four of the proteins are components of the extracellular matrix (ECM), and increases in certain ECM proteins occur in fibrosis. The last two are involved in insulin signal transduction; one of them, IGFBP1, increases in the serum during alcohol consumption.[24]

To determine whether the biological processes we inferred from the expression data occurred more often than chance in our lists of expressed proteins, a gene ontology analysis was performed using the DAVID 2008 functional annotation tool.[19,20] Only two clusters of genes associated with ontology terms were statistically significantly overrepresented in the data set. The top-scoring cluster was associated with the term "alcohol catabolic process" (GO:0046164; FDR = 2.16×10^{-6}) and included eight proteins (ALDOA, ALDOC, ENO1, LDHA, MDH1, PGAM, PGK1, and TPI1). This term refers to the breakdown of any compound containing a hydroxyl group attached to a saturated carbon-not just ethanol-and includes glucose catabolism as a child term. The next highest-scoring set included six proteins (C4A, C4B, CLU, ORM2, SERPINA3, and TF) described by the term "acute inflammatory response" (GO:0002526; FDR = 0.0092). The "regulation of programmed cell death" (GO:0043067) term describing eight proteins (APOE, CFL1, CLU, HSPD1, HSPE1, MIF, NME1, and NME2) and the "acute-phase response" term (GO:0006953) including three proteins (ORM2, SERPINA3, and TF) were the next highest-scoring set, but neither met significance criteria with the Benjamini multitest correction (FDR < 0.05).

Quantification of Proteins. To partly verify the detected changes in the abundance of proteins and to extend the analysis of our system's physiological similarity to known responses to ethanol toxicity, we performed a slide-based, multiplexed enzyme-linked immunosorbent assay (ELISA) for eight proteins (Figure 2). Two of these (IGFBP1 and MIF) were among the proteins that increased in abundance in the mass spectrometry study, and both of their increases were confirmed in medium from the high-ethanol concentration condition ($p = 0.036$ and $p = 0.005$, respectively), though only IGFBP1 was shown to be increased significantly at the low-ethanol con-

Table 4. Extracellular Proteins Changing in Abundance[a]

symbol	name	biological role	200 mM	500 mM
APOA1	Apolipoprotein A-I	Acute-phase response	3.65	3.95
APOH	Apolipoprotein H	Acute-phase response	1.76	2.76
SERPINF1	Serpin peptidase inhibitor, clade F, member 1 (pigment epithelium derived factor)	Acute-phase response	2.78	2.72
TF	Transferring	Acute-phase response		EtOH Only
C4	Complement component 4	Acute-phase response; inflammatory response	1.90	1.67
ORM2	Orosomucoid 2	Acute-phase response; inflammatory response	0.72	0.46
SERPINA3	Serpin peptidase inhibitor, clade A, member 3 (antichymotrypsin)	Acute-phase response; inflammatory response	6.02	2.80
APOE	Apolipoprotein E	Inflammatory response; regulation of apoptosis	2.34	2.76
CLU	Clusterin	Inflammatory response; regulation of apoptosis	1.32	2.49
GDF15	Growth differentiation factor 15	Inflammatory response; regulation of apoptosis	1.33	3.92
MIF	Macrophage migration inhibitory factor	Inflammatory response; regulation of apoptosis	1.42	8.78
CTGF	Connective tissue growth factor	Proteinaceous extracellular matrix	1.01	1.81
FBLN1	Fibulin 1	Proteinaceous extracellular matrix	1.26	1.94
LGALS3BP	Galectin 3	Proteinaceous extracellular matrix	1.23	2.23
MATN3	Matrilin 3	Proteinaceous extracellular matrix	0.99	0.53
IGF2	Insulin-like growth factor 2	Insulin signal transduction	1.13	1.75
IGFBP1	Insulin-like growth factor binding protein 1	Insulin signal transduction	1.57	2.28

[a] Proteins collected from the conditioned medium of HepG2/C3A cells treated with 200 mM ethanol, 500 mM ethanol, or as control were analyzed by LC−MS^E. Proteins changing in abundance by 1.5-fold from control or identified in all four replicates of one condition but no replicates of another and annotated as being extracellular were selected. HGNC gene symbols and ratios of fold change versus control for 200 or 500 mM ethanol exposure are indicated. Proteins indentified only in exposed samples are indicated as "EtOH Only" when present in all four replicates or as the number of replicates (rep) that the protein was identified in.

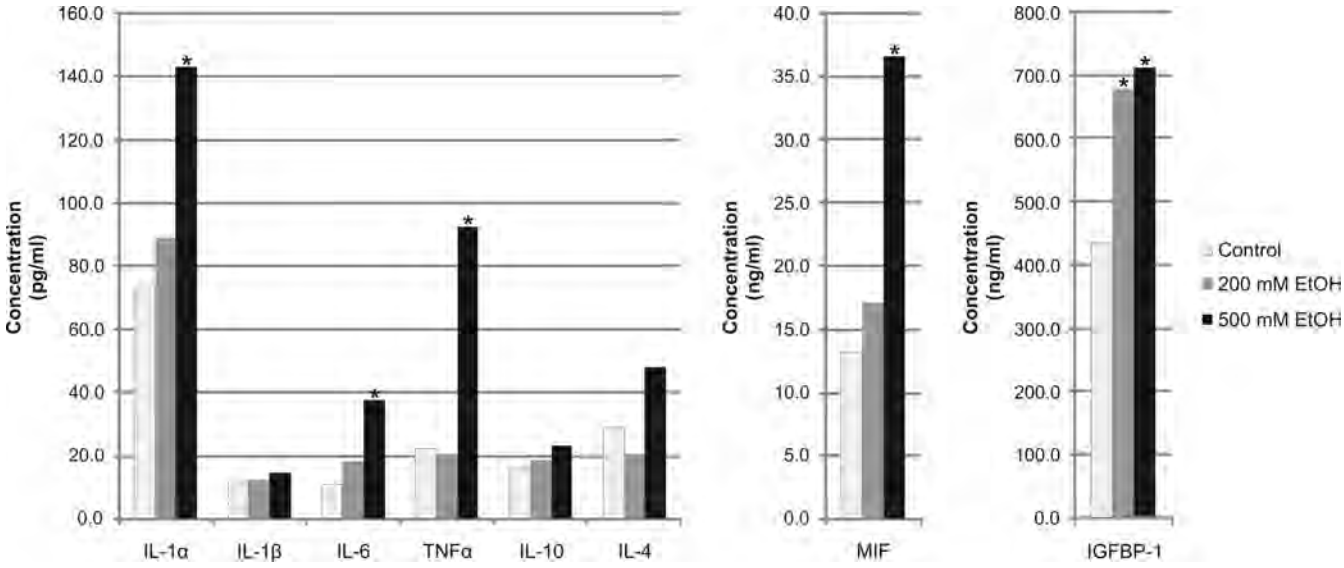

Figure 2. Multiplex ELISA of select proteins. Proteins from the conditioned medium of HepG2/C3A cells treated with 200 mM ethanol, 500 mM ethanol, or as control were collected after 24 h. Concentrations of proteins were determined using a slide-based multiplex ELISA. Conditions significantly different from controls ($p < 0.05$) are indicated with an asterisk.

centration ($p = 0.001$). Three of the six other cytokines (IL-1α, IL-6, and TNFα) increased in response to the high-ethanol treatment with respect to control ($p = 0.034$, $p = 0.009$, and $p = 0.023$, respectively). Interestingly, these are known pro-inflammatory cytokines and are the key cytokine regulators of the acute-phase signaling pathway.[26] Although IL-1α and IL-1β can play similar biological roles, they are differentially regulated, as IL-1β is not up-regulated.

Discussion

The identification of proteins directly secreted from cells or tissue in response to exposure to a toxicant is a powerful approach for the discovery of biomarkers of toxicity. The human hepatoma cell line, HepG2/C3A, appears to be a suitable *in vitro* model for investigating liver toxicity and identifying potential biomarkers of liver insult. In this work, we identified proteins in the extracellular space that change in abundance as a result of ethanol exposure. Some of them are merely indicators of cell death and the consequent release of intracellular polypeptides, but many match known effects of ethanol exposure and alcoholism.

Model Consistent with Known Effects. An important consideration with any *in vitro* model system is that responses are consistent with *in vivo* effects. The HepG2/C3A cell line cultured in MED6 has been tested as a model of hepatoxicity and has shown to have a high concordance with human liver cells[7,8] (http://www.activtox.com). In fact, this cell line has been used in the clinical trial of a liver assist device for temporarily

supporting individuals awaiting liver transplants.[10] In our study, all of the proteins changing in abundance are consistent with known effects of ethanol toxicity ranging from apoptosis and inflammation to cell leakage from disrupted cells. Two proteins, macrophage migration inhibitory factor (MIF) and insulin-like growth factor binding protein 1 (IGFBP1), whose secretion increased in response to ethanol exposure, are upregulated in response to alcoholic liver disease or ethanol exposure.[24,27]

Cytokine Response. We measured the levels of IL-1α, IL-6, and TNFα in medium, and they were increased in the highest treatment. These cytokines have been previously shown to be upregulated in alcoholism.[28] They are all pro-inflammatory cytokines and mediators of the acute-phase response. This observation corresponds well with the changes in secretion of a large number of acute-phase and inflammatory proteins. However, several of the proteins (APOA1, APOH, and TF) are negative acute-phase serum proteins, yet in this work their abundance is increased. This discrepancy could represent a failure in gene regulation in the HepG2/C3A cell line or might also reflect the requirement for an additional cell type for proper acute-phase response signaling. IL-1, IL-6, and TNFα are primarily secreted by macrophages *in vivo*.

Nutritional Effects. While many of the observed effects appear to result from damage to the cells, ethanol can also be a source of energy. Two proteins, IGF1 and IGFBP1, were present at a higher abundance in medium from exposed cells than in controls and are involved in the insulin pathway. At least one, IGFBP1, has been shown to be upregulated in response to ethanol exposure though its induction appears to be partly mediated by TNFα and possibly by IL-1.[29,30] Although cell leakage is the obvious explanation for the increased abundance of the glycolytic enzymes in medium from exposed cells, the levels of some of the enzymes might also be increased as metabolic adaptation, which might partially explain why the levels of elevation are different among these enzymes at the high dose (Table 3).

Extracellular Matrix. Ethanol-induced liver damage includes fibrosis, which is characterized by an increase in certain extracellular matrix (ECM) proteins, primarily type I and III collagen, but also proteoglycans, fibronectin, and elastin.[31,32] In the liver, collagen proteins are produced by hepatic stellate cells (HSCs), which are not present in this *in vitro* model. In ethanol-treated cells, the increased secretion of four ECM-related proteins (CTGF, FBLN1, MATN3, and LGALS3BP) is consistent with fibrotic effects and could represent changes to the hepatocytes within the liver. We find increased secretion of ECM-binding proteins such as LGALS3BP and FBLN1. CTGF, which mediates ECM production, is produced not only by HSCs in fibrotic livers but also by hepatocytes in response to ethanol oxidation.[33] At least one matrilin, MATN2, has been shown to be upregulated in cirrhosis.[34] While the matrilin identified in this work, MATN3, is not typically expressed in the liver,[35] its increase in the context of the other indicators of ECM changes supports the observation of a fibrotic effect but obviously represents a difference in gene regulation between hepatocytes and these cells. However, taken together, the changes in ECM-related proteins signify that at least part of the response to ECM rearrangement and fibrosis is being seen in the HepG2/C3A model.

Cell Leakage. The largest confounding effect in this model system is the presence of leaked proteins in the medium since they are not inherently toxicologically interesting. At toxicant concentrations that cause cell death, large numbers of cytosolic proteins are present in the medium. In the 500 mM ethanol-exposed samples, for example, nearly all of the enzymes in the glycolytic pathway were detected. In fact, even under control conditions, intracellular proteins have been seen in the medium by us and others using HepG2 cells,[36,37] presumably due to some basal level of cell death. The challenge in interpreting this data is that some of these proteins changing in abundance at the high-concentration level may be secreted by nonclassical pathways and are relevant as biomarkers. Several intracellular proteins are likely to be upregulated based on the known mechanisms of ethanol toxicity, so changes in their abundance in the medium are unlikely to be wholly a consequence of cell leakage. However, for identification of novel changes, a more effective means of controlling for leaked proteins is required.

Future work using this model will need to include a robust method for calibrating tissue leakage markers (such as LDH) to ensure that multiple toxicants are exposed at similar cytotoxic levels. Also, several unrelated toxicants will need to be compared simultaneously to clarify which proteins in the secretome simply represent nonspecific effects of stress or cell death. With concentrations chosen to create equal levels of cell leakage, identification of proteins that are differentially affected by various toxicants will be possible. On a side note, we have observed that commercially available LDH assays rely on a reduction reaction that can easily be interfered with by certain chemicals (for example, sodium dichromate; unpublished data). Different methods of measuring cytotoxicity might be required to ensure reliability across a variety of chemical types.

Limitations of Model. The single largest shortcoming of any *in vitro* model is the lack of complex intercellular interactions that are present *in vivo*. Several of the known mechanisms of ALD progression require the interaction of multiple cell types. For example, inflammation and the cytokine response is mediated through macrophage cells, and the increase in extracellular matrix deposition (see "Extracellular matrix" above) requires HSCs. Furthermore, diseases like alcoholism can affect multiple organs. It has been shown that alcohol consumption can stimulate the release of LPS by the gut leading to a sensitization to the cytokine response in the liver.[12]

It is commonly accepted that immortalized cell lines do not fully mimic the gene expression of *in vivo* cells. In hepatocyte-derived cells, biologically significant differences from primary cells include the levels of bioactivating enzyme activity and a mature liver phenotype. To address this problem with immortalized cells at least in part, we chose to use a cell line (HegG2/C3A) that has a phenotypic change at confluence that includes an increase in the ALB/AFP ratio and a decrease in fetal enzyme isoforms.[7,8] It can also bioactivate a range of toxicants,[9] (http://www.activtox.com). Although this work was performed under culture conditions meant to optimize this phenotype, there were still detectable levels of ALDOA and ALDOC, whose expression is replaced by ALDOB in mature liver cells, and AFP, indicating that a fully mature liver phenotype has not been achieved. Furthermore, not all gene expression mimicked predicted models; for example, several negative acute-phase proteins were upregulated. When choosing toxicants and evaluating results, care must be taken to ensure that limitations of the system are considered.

A significant difficulty in all proteomics experiments is dealing with the potential large dynamic range of protein concentrations. This model helps to maximize concentrations of proteins of interest to help overcome this challenge, but the ability of available methods to measure low-abundance pro-

teins in discovery experiments is still limited. In this study, AFP is the most abundant protein (1−10 μg/mL, unpublished data) after immunodepletion. The least abundant protein that was identified by mass spectrometry and for which an absolute concentration is known is MIF (∼10 ng/mL). This represents a dynamic range of 2−3 orders of magnitude. Unfortunately, some critical proteins such as cytokines are present at 10−100 pg/mL concentrations. To be able to quantify the AFP and cytokines in the same experiment, 6 orders of magnitude would be required. This is beyond the capabilities of current mass spectrometry technology.

While immunodepletion plays a key role in enhancing the dynamic range of proteomic analyses, some proteins of interest may not be completely retained on the column and others may also be unexpectedly adsorbed. We were surprised to find transferrin in the flow-through from the immunodepletion column and three nonspecific proteins in the bound fraction. In the future this problem might be resolved by the development of a column tuned to the concentration of proteins in the secretome which could provide a more comprehensive immunodepletion with less nonspecific binding.

Conclusions

We have shown that proteins secreted from HepG2/C3A cells can be successfully identified and quantified using standard LC/MS^E techniques. A total of 87 proteins were identified for which 37 exhibited changes in abundance due to ethanol exposure. The differences in secreted protein abundances we observed are consistent with known mechanisms of ethanol toxicity and include apoptosis, inflammation, acute-phase response, and increase in ECM proteins. The use of immunodepletion techniques designed for serum enhanced the depth of coverage and number of protein identifications, but they may potentially remove some proteins nonspecifically. Though there are potential limitations with this system, this model provides a useful tool for rapid identification of potential markers of toxic exposure.

Acknowledgment. Opinions, interpretations, conclusions, and recommendations are those of the authors and are not necessarily endorsed by the U.S. Army. The research was sponsored by the U.S. Army Medical Research and Materiel Command, Military Operational Medicine Research Program. Citations of commercial organizations or trade names in this report do not constitute an official Department of the Army endorsement or approval of the products or services of these organizations. The authors wish to thank Dr. Naissan Hussainzada and Dr. James Dillman for critical review of the manuscript.

Supporting Information Available: List of identified peptides, protein identification data for the bound fraction, and protein identification and quantification data for the immunodepleted protein fraction. This material is available free of charge via the Internet at http://pubs.acs.org.

References

(1) Rifai, N.; Gillette, M. A.; Carr, S. A. Protein biomarker discovery and validation: the long and uncertain path to clinical utility. *Nat. Biotechnol.* **2006**, *24*, 971–983.

(2) *Liver Disease Subcommittee of the Digestive Diseases Interagency Coordinating Committee. Action Plan for Liver Disease Research*; National Institutes of Health: Bethesda, MD, 2004; pp 87−93.

(3) Hewitt, N. J.; Lechon, M. J.; Houston, J. B.; Hallifax, D.; Brown, H. S.; Maurel, P.; Kenna, J. G.; Gustavsson, L.; Lohmann, C.; Skonberg, C.; Guillouzo, A.; Tuschl, G.; Li, A. P.; LeCluyse, E.; Groothuis, G. M.; Hengstler, J. G. Primary hepatocytes: current understanding of the regulation of metabolic enzymes and transporter proteins, and pharmaceutical practice for the use of hepatocytes in metabolism, enzyme induction, transporter, clearance, and hepatotoxicity studies. *Drug Metab. Rev.* **2007**, *39*, 159–234.

(4) Flynn, T. J.; Ferguson, M. S. Multiendpoint mechanistic profiling of hepatotoxicants in HepG2/C3A human hepatoma cells and novel statistical approaches for development of a prediction model for acute hepatotoxicity. *Toxicol. in Vitro* **2008**, *22*, 1618–1631.

(5) Westerink, W. M.; Schoonen, W. G. Phase II enzyme levels in HepG2 cells and cryopreserved primary human hepatocytes and their induction in HepG2 cells. *Toxicol. in Vitro* **2007**, *21*, 1592–1602.

(6) Westerink, W. M.; Schoonen, W. G. Cytochrome P450 enzyme levels in HepG2 cells and cryopreserved primary human hepatocytes and their induction in HepG2 cells. *Toxicol. in Vitro* **2007**, *21*, 1581–1591.

(7) Kelly, J. H.; Darlington, G. J. Modulation of the liver specific phenotype in the human hepatoblastoma line Hep G2. *In Vitro Cell. Dev. Biol.* **1989**, *25*, 217–222.

(8) Kelly, J. H. Permanent human hepatocyte cell line and its use in a liver assist device (LAD). United States Patent No. 5, 1994; pp 290−684.

(9) Kelly, J. H.; Sussman, N. L. A fluorescent cell-based assay for cytochrome P- 450 isozyme 1A2 induction and inhibition. *J. Biomol. Screen* **2000**, *5*, 249–254.

(10) Gislason, G. T.; Lobdell, D. D.; Kelly, J. H.; Sussman, N. L. A treatment system for implementing an extracorporeal liver assist device. *Artif. Organs* **1994**, *18*, 385–389.

(11) De Minicis, S.; Brenner, D. A. Oxidative stress in alcoholic liver disease: role of NADPH oxidase complex. *J. Gastroenterol. Hepatol.* **2008**, *23*, S98–103.

(12) Schaffert, C. S.; Duryee, M. J.; Hunter, C. D.; Hamilton, B. C., III; DeVeney, A. L.; Huerter, M. M.; Klassen, L. W.; Thiele, G. M. Alcohol metabolites and lipopolysaccharide: roles in the development and/or progression of alcoholic liver disease. *World J. Gastroenterol.* **2009**, *15*, 1209–1218.

(13) Albano, E. New concepts in the pathogenesis of alcoholic liver disease. *Expert Rev. Gastroenterol. Hepatol.* **2008**, *2*, 749–759.

(14) Hammel, P.; Couvelard, A.; O'Toole, D.; Ratouis, A.; Sauvanet, A.; Flejou, J. F.; Degott, C.; Belghiti, J.; Bernades, P.; Valla, D.; Ruszniewski, P.; Levy, P. Regression of liver fibrosis after biliary drainage in patients with chronic pancreatitis and stenosis of the common bile duct. *N. Engl. J. Med.* **2001**, *344*, 418–423.

(15) Vozar, I. Serum laboratory markers for noninvasive diagnosis and monitoring of liver fibrogenesis in patients with chronic liver diseases. *Bratisl. Lek. Listy* **2005**, *106*, 123–126.

(16) Geromanos, S. J.; Vissers, J. P.; Silva, J. C.; Dorschel, C. A.; Li, G. Z.; Gorenstein, M. V.; Bateman, R. H.; Langridge, J. I. The detection, correlation, and comparison of peptide precursor and product ions from data independent LC-MS with data dependant LC-MS/MS. *Proteomics* **2009**, *9*, 1683–1695.

(17) Li, G. Z.; Vissers, J. P.; Silva, J. C.; Golick, D.; Gorenstein, M. V.; Geromanos, S. J. Database searching and accounting of multiplexed precursor and product ion spectra from the data independent analysis of simple and complex peptide mixtures. *Proteomics* **2009**, *9*, 1696–1719.

(18) Silva, J. C.; Gorenstein, M. V.; Li, G. Z.; Vissers, J. P.; Geromanos, S. J. Absolute quantification of proteins by LCMSE: a virtue of parallel MS acquisition. *Mol. Cell. Proteomics* **2006**, *5*, 144–156.

(19) Dennis, G.; Sherman, B. T.; Hosack, D. A.; Yang, J.; Gao, W.; Lane, H. C.; Lempicki, R. A. DAVID: Database for Annotation, Visualization, and Integrated Discovery. *Genome Biol.* **2003**, *4*, P3.

(20) Huang, D. W.; Sherman, B. T.; Lempicki, R. A. Systematic and integrative analysis of large gene lists using DAVID bioinformatics resources. *Nat. Protoc.* **2009**, *4*, 44–57.

(21) Betts, G. F.; Srivastava, D. K. The rationalization of high enzyme concentration in metabolic pathways such as glycolysis. *J. Theor. Biol.* **1991**, *151*, 155–167.

(22) Baulac, S.; Lu, H.; Strahle, J.; Yang, T.; Goldberg, M. S.; Shen, J.; Schlossmacher, M. G.; Lemere, C. A.; Lu, Q.; Xia, W. Increased DJ-1 expression under oxidative stress and in Alzheimer's disease brains. *Mol. Neurodegener.* **2009**, *4*, 12.

(23) Reinecke, F.; Levanets, O.; Olivier, Y.; Louw, R.; Semete, B.; Grobler, A.; Hidalgo, J.; Smeitink, J.; Olckers, A.; Van der Westhuizen, F. H. Metallothionein isoform2A expression is inducible and protects against ROS-mediated cell death in rotenone-treated HeLa cells. *Biochem. J.* **2006**, *395*, 405–415.

(24) Röjdmark, S.; Rydvald, Y.; Aquilonius, A.; Brismar, K. Insulin-like growth factor (IGF)- 1 and IGF-binding protein-1 concentrations in serum of normal subjects after alcohol ingestion: evidence for decreased IGF-1 bioavailability. *Clin. Endocrinol. (Oxford)* **2000**, *52*, 313–318.
(25) McClain, C. J.; Song, Z.; Barve, S. S.; Hill, D. B.; Deaciuc, I. Recent advances in alcoholic liver disease. IV. Dysregulated cytokine metabolism in alcoholic liver disease. Am J Physiol Gastrointest. *Liver Physiol.* **2004**, *287*, G497–G502.
(26) Heinrich, P. C.; Castell, J. V.; Andus, T. Interleukin-6 and the acute phase response. *Biochem. J.* **1990**, *265*, 621–636.
(27) Kumagi, T.; Akbar, F.; Horiike, N.; Onji, M. Increased serum levels of macrophage migration inhibitory factor in alcoholic liver diseases and their expression in liver tissues. *Clin. Biochem.* **2001**, *34*, 189–193.
(28) Khoruts, A.; Stahnke, L.; McClain, C. J.; Logan, G.; Allen, J. I. Circulating tumor necrosis factor, interleukin-1 and interleukin-6 concentrations in chronic alcoholic patients. *Hepatology* **1991**, *13*, 267–276.
(29) Kumar, V.; Silvis, C.; Nystrom, G.; Deshpande, N.; Vary, T. C.; Frost, R. A.; Lang, C. H. Alcohol-induced increases in insulin-like growth factor binding protein-1 are partially mediated by TNF. *Alcohol.: Clin. Exp. Res.* **2002**, *26*, 1574–1583.
(30) Lang, C. H.; Nystrom, G. J.; Frost, R. A. Regulation of IGF binding protein-1 in hep G2 cells by cytokines and reactive oxygen species. *Am. J. Physiol.* **1999**, *276*, G719–G727.
(31) Gressner, A. M.; Bachem, M. G. Cellular sources of noncollagenous matrix proteins: role of fat-storing cells in fibrogenesis. *Semin. Liver Dis.* **1990**, *10*, 30–46.
(32) Friedman, S. L. Seminars in medicine of the Beth Israel Hospital, Boston. The cellular basis of hepatic fibrosis. Mechanisms and treatment strategies. *N. Engl. J. Med* **1993**, *328*, 1828–1835.
(33) Rachfal, A. W.; Brigstock, D. R. Connective tissue growth factor (CTGF/CCN2) in hepatic fibrosis. *Hepatol. Res.* **2003**, *26*, 1–9.
(34) Szabó, E.; Korpos, E.; Batmunkh, E.; Lotz, G.; Holczbauer, A.; Kovalszky, I.; Deak, F.; Kiss, I.; Schaff, Z.; Kiss, A. Expression of matrilin-2 in liver cirrhosis and hepatocellular carcinoma. *Pathol. Oncol. Res.* **2008**, *14*, 15–22.
(35) Klatt, A. R.; Nitsche, D. P.; Kobbe, B.; Morgelin, M.; Paulsson, M.; Wagener, R. Molecular structure and tissue distribution of matrilin-3a filament-forming extracellular matrix protein expressed during skeletal development. *J. Biol. Chem.* **2000**, *275*, 3999–4006.
(36) Yamashita, R.; Fujiwara, Y.; Ikari, K.; Hamada, K.; Otomo, A.; Yasuda, K.; Noda, M.; Kaburagi, Y. Extracellular proteome of human hepatoma cell, HepG2 analyzed using two-dimensional liquid chromatography coupled with tandem mass spectrometry. *Mol. Cell. Biochem.* **2007**, *298*, 83–92.
(37) Higa, L. M.; Caruso, M. B.; Canellas, F.; Soares, M. R.; Oliveira-Carvalho, A. L.; Chapeaurouge, D. A.; Almeida, P. M.; Perales, J.; Zingali, R. B.; Da Poian, A. T. Secretome of HepG2 cells infected with dengue virus: implications for pathogenesis. *Biochim. Biophys. Acta* **2008**, *1784*, 1607–1616.

PR1005668